30 August 1996

ELSEVIER

Chemical Physics Letters 259 (1996) 81–90

CHEMICAL PHYSICS LETTERS

Assigning vibrational spectra of highly excited molecules: classical and quantum vibrational dynamics of the H_2O molecule

Srihari Keshavamurthy, Gregory S. Ezra

Baker Laboratory, Department of Chemistry, Cornell University, Ithaca, NY 14853, USA

Received 2 April 1996; in final form 11 June 1996

Abstract

We study the classical and quantum mechanics of the 3-mode Baggot vibrational Hamiltonian for H_2O. Chirikov resonance analysis gives an approximate view of the classical phase space structure. Computation of periodic orbits and families of resonant 2-tori provides a more rigorous basis for the use of the Chirikov picture. Examination of classical surfaces of section together with quantum mechanical Husimi phase space distribution functions leads to a dynamical assignment of almost all 45 states considered. The most extensive mixing occurs via a 2-state avoided crossing.

1. Introduction

Understanding the nature of highly excited vibrational and rotation–vibration states of polyatomic molecules is a problem of central importance in chemical physics. Traditional spectroscopic methods for assignment of levels based on harmonic oscillator (normal mode)-rigid rotor quantum numbers and wavefunctions can break down for highly excited rovibrational states as a result of strong mode coupling [1,2]. Such mode coupling, due either to anharmonic coupling terms in the potential or to rotation-vibration interaction, leads to the phenomenon of intramolecular vibrational energy redistribution (IVR) [2], and results in complicated energy level and intensity patterns.

One source of apparent complexity in vibrational spectra is strong mixing of manifolds of near-degenerate states by a single resonant coupling term; the corresponding classical problem is nevertheless integrable in this case. Another possibility is strong mixing of states due to the presence of two or more resonant coupling terms; classically, the problem is nonintegrable and we have the possibility of chaos [3]. State mixing can also occur as a result of *dynamical tunneling* [4], a nonclassical mixing of states localized in different regions in phase space that is associated either with symmetry related or accidental degeneracies of levels.

Many approaches have been proposed for the study of complicated spectra beyond traditional methods [5–10]. Considerable progress has been made in the analysis of two modes coupled by a single resonant term [9]. In this case there is a constant of the motion in addition to the total energy, and the associated reduced phase space is a 2D *sphere*, the so-called polyad phase sphere [11,12]. Classically, one can study the fixed points of a reduced 1 degree-of-freedom (dof) spectroscopic Hamiltonian on the sphere, which correspond to periodic orbits (pos) in the full phase space. These fundamental periodic orbits serve as organizing centers for the classical and quantum phase space. As parameters such as energy or polyad number are changed, these periodic orbits will bifurcate or merge,

PII S0009-2614(96)00727-0

leading to qualitative changes in the phase space structure. Each distinct arrangement of periodic orbits and associated stable and unstable manifolds (for unstable pos) defines a *zone* in parameter space, and Kellman and coworkers (see Ref. [9] and references therein) have systematically studied the bifurcation of pos and the passage from one zone to another for both 1:1 and 2:1 resonant systems (see also Ref. [13]). Periodic orbit bifurcations in 1:1 and 2:1 resonant vibrational Hamiltonians have also been studied using semiclassical energy-time analysis of level spectra [14].

It is of considerable interest to attempt to extend the above approach to deal with multi-mode ($N \geqslant 3$) systems. More generally, we seek to develop qualitative methods for analysis of energy level patterns and wavefunctions in multimode systems based on the underlying classical nonlinear dynamics. One possibility is to determine pos for multimode Hamiltonians. Lu and Kellman [15] have recently examined pos and their bifurcations in a classical version of the 3-mode vibrational spectroscopic Hamiltonian for H_2O due to Baggot [16]. The Baggot Hamiltonian [16] has an extra constant of the motion in addition to the energy, the so called superpolyad number $\mathcal{N} = 2(n_1+n_2)+n_b$ (see next section). In the presence of this additional constant of the motion, the Baggot Hamiltonian has essentially 2 degrees of freedom. Following the procedure used for 2-mode resonant problems, Lu and Kellman have determined critical points of the 2-mode reduced Hamiltonian for H_2O; these critical points correspond to periodic orbits in the full phase space [15,17]. One can then attempt to use the pos as a framework for organizing the phase space structure and to understand the localization of quantum eigenstates.

An important aspect of the study of the phase space structure of multimode systems is the search for ways to partition (either approximately or exactly) phase space (full or reduced, at constant E) into regions corresponding to qualitatively different dynamics. In the case that the Hamiltonian of interest has two degrees of freedom, the stable and unstable manifolds of unstable pos have the appropriate dimensionality to divide the energy shell into disjoint regions, and each zone in parameter space is then associated with a different partitioning of the polyad phase sphere [9]. Such partitions have been used in theories of phase space transport in systems with mixed phase space [18,19]. The relevant pos can be determined either as critical points on the polyad phase sphere for the case of a single resonant coupling, or as fixed points on a Poincaré section. For $N \geqslant 3$ mode systems, however, the stable and unstable manifolds of unstable pos do not have sufficiently high dimension to define a partition of phase space (for a detailed discussion of dimensionality issues of dividing surfaces in multimode systems, see Ref. [20]).

A *resonance channel* or resonance zone is a region of phase space of full dimensionality consisting of trajectories that are strongly affected by a coupling term in the Hamiltonian corresponding to a single resonance condition on N zeroth-order frequencies [3]. In an integrable N degree of freedom system, a single resonance condition $\boldsymbol{m} \cdot \boldsymbol{\Omega}(\boldsymbol{I}) = 0$ can be satisfied on a continuous $(N-2)$-parameter family of N-tori on the $(2N-1)$-D energy shell, $E = H$. Under the influence of the associated resonant coupling term, each N-torus in general breaks up into a number of pairs of $(N-1)$-tori, where one member of each pair is a "whiskered" $(N-1)$-torus with N-dimensional stable and unstable manifold [19]. The stable and unstable manifolds of the $N-2$ parameter family of resonant $(N-1)$-tori are $2N-2$ dimensional, and have the right dimension to divide the $2N-1$ dimensional energy surface into disjoint regions. In the case that the stable and unstable manifolds join smoothly, as in the single resonance case, they naturally define the boundary of the resonance channel, with an "inside" and an "outside". In the case that additional perturbations are present, the stable and unstable manifolds may still intersect transversely, in which case the boundary of the resonance zone is formed by taking appropriate segments of the stable and unstable manifolds, but is no longer an invariant surface [3,19]. In this case the stable and unstable manifolds can be determined numerically, although with considerable difficulty [20].

The key point is that resonance channels define regions of phase space characterized by particular dynamical behavior; it is therefore natural to use them as the basis for a partitioning of phase space in multimode systems. The totality of resonance channels forms the Arnold web [21]. Phase points can drift along resonance channels, and "change direction" at intersections between channels [3].

The location and width of resonance channels in a given system can be determined approximately using

the standard analysis due to Chirikov [22]. In their pioneering work, Oxtoby and Rice mapped out resonance zones for 2- and multi-mode model molecular Hamiltonians in order to correlate the onset of resonance overlap with statistical unimolecular decay dynamics [23]. Resonance channels have since been mapped out for a number of molecular Hamiltonians (see, for example Refs. [24–29]), and connections with the corresponding quantum systems examined [27–29]. Of particular interest in multimode classical systems is the possibility of chaotic motion at the intersection of resonance channels [25,28,30].

In the present Letter we examine the problem of assigning highly excited quantum states of the 3-mode Baggot Hamiltonian for H_2O. Our approach is based upon a close study of the classical–quantum correspondence, taking as our starting point a Chirikov analysis of the resonance channels [22]. Chirikov's method is an approximate, perturbative approach to the phase space structure of multimode systems, in that the different resonances are analyzed independently. It is however possible to refine the Chirikov resonance analysis by determining the location of families of resonant $(N-1)$-tori (2-tori in the case of the 3-mode Baggot hamiltonian) determined in the single resonance approximation. We find that the results of the elementary Chirikov analysis and the more refined analysis are in close agreement, confirming the essential correctness of the Chirikov picture. We study the classical–quantum correspondence via the Husimi distribution function [31] for eigenstates of the Baggot Hamiltonian. The Husimi functions together with the resonance analysis enable us to give a dynamical assignment for almost all states in the $P = 8$ manifold. The most extensive mixing occurs via a 2-state avoided crossing.

In Section 2 we describe the classical and quantum versions of the Baggot Hamiltonian for H_2O [16]. Section 3 provides a brief survey of the classical phase space structure of the classical Baggot Hamiltonian. The locations of resonance zones, families of 2-tori, and periodic orbits are discussed. We also describe a useful Poincaré section that provides a global view of the classical phase space structure. In Section 4 we examine phase space distribution functions for eigenstates of the Baggot Hamiltonian in light of the classical–quantum correspondence. Eigenstate assignment, localization and the nature of "mixed" states are discussed. Section 5 concludes.

2. Baggot Hamiltonian for H_2O

2.1. Classical Hamiltonian

The classical version of the spectroscopic Hamiltonian for H_2O derived by Baggot [16] is a three degree of freedom local mode Hamiltonian which includes two 2:1 stretch–bend resonant terms $\mathcal{H}_\sigma^{2:1}$, $\sigma = 1$ or 2, a 1:1 stretch–stretch resonant term $\mathcal{H}^{1:1}$ and a 2:2 stretch–stretch term $\mathcal{H}^{2:2}$:

$$\mathcal{H} = \mathcal{H}_0 + \mathcal{H}^{1:1} + \mathcal{H}^{2:2} + \sum_{\sigma=1,2} \mathcal{H}_\sigma^{2:1} , \tag{2.1}$$

where $\mathcal{H}_0$ is the zeroth order Hamiltonian

$$\mathcal{H}_0 = \Omega_s \sum_{\sigma=1,2} I_\sigma + \Omega_b I_b + \alpha_s \sum_{\sigma=1,2} I_\sigma^2 + \alpha_b I_b^2 + \epsilon_{ss} I_1 I_2 + \epsilon_{sb} I_b \sum_{\sigma=1,2} I_\sigma , \tag{2.2}$$

and the resonant interaction terms are

$$\mathcal{H}^{1:1} = \beta'_{12} (I_1 I_2)^{1/2} \cos(\theta_1 - \theta_2), \tag{2.3a}$$

$$\mathcal{H}^{2:2} = \beta_{22} I_1 I_2 \cos[2(\theta_1 - \theta_2)], \tag{2.3b}$$

$$\mathcal{H}_\sigma^{2:1} = \beta_{sb} (I_\sigma I_b^2)^{1/2} \cos(\theta_\sigma - 2\theta_b). \tag{2.3c}$$

Here, $(\{I_s, \theta_s\}, I_b, \theta_b) \equiv (\boldsymbol{I}, \boldsymbol{\theta})$ are canonical action-angle variables for the two local mode stretches and the bend mode, respectively, and $\beta'_{12} \equiv \beta_{12} + \lambda'(I_1 + I_2) + \lambda'' I_b$, with $\beta_{12}, \lambda'' < 0$ and $\lambda' > 0$ [16].

It is important to note that the resonance vectors $(1, -1, 0)$, $(1, 0, -2)$ and $(0, 1, -2)$ are linearly dependent [32,33], so that there is a constant of the motion $\mathcal{N}$ in addition to the energy:

$$\mathcal{N} = 2 \sum_{\sigma=1,2} I_\sigma + I_b. \tag{2.4}$$

Conservation of $\mathcal{N}$ means that we can follow the classical evolution of action variables for given $(\mathcal{N}, E)$ in the two-dimensional action plane (I_1, I_2).

It turns out that the 2:2 stretch–stretch resonance (Darling–Dennison coupling) does not significantly affect the classical phase space structure in the regime

of interest for this Letter, and it is omitted from the Hamiltonian in the resonance analysis described below. It is however straightforward to include this coupling term if required.

2.2. Quantum Hamiltonian

The quantum version of the Baggot Hamiltonian is obtained via the standard correspondence between action–angle variables and creation–annhilation operators:

$$\hat{a}^{\dagger} \leftrightarrow I^{1/2} e^{i\theta}, \quad \hat{a} \leftrightarrow I^{1/2} e^{-i\theta}. \tag{2.5}$$

Using the above correspondence and expressing the resultant Hamiltonian in a basis of number states $|n_1 n_2 n_b\rangle$, we obtain Baggot's Hamiltonian [16] with the following mapping of parameters:

$$(\beta_{12}, \beta_{22}, \lambda', \lambda'') \leftrightarrow 2(\lambda, \gamma, \lambda', \lambda''),$$
$$\beta_{sb} \leftrightarrow \frac{1}{\sqrt{2}} k_{sbb}, \tag{2.6}$$

where λ and k_{sbb} are defined in Ref. [16]. Values of the various parameters are taken from Baggot's fit to the vibrational levels of H_2O (Table 2 of Ref. [16]).

The *superpolyad number*, $P = \sum_{\sigma=1,2} n_s + n_b/2$, is a constant of the motion for the quantum Baggot Hamiltonian. A given value of P is associated with a corresponding classical invariant $\mathcal{N} = 2P + \frac{5}{2}$.

3. Classical mechanics of 3-mode H_2O

In this section we provide a brief overview of the classical mechanics of the 3-mode Baggot vibrational H_2O Hamiltonian. For more details, see Ref. [34]. The results of our analysis are summarized in Fig. 1, which shows the classical phase space structure in the (I_1, I_2) plane for $\mathcal{N} = 18.5$ ($P = 8$). Fig. 1 shows contours of $\mathcal{H}_0$, the location of periodic orbits, resonance channels, and families of resonant 2-tori.

3.1. Periodic orbits and their bifurcations

In studying the phase space structure of H_2O, a first step is the determination of the primary *periodic orbits*. For a 3-mode system with 2 linearly independent resonance coupling vectors, these pos can be located

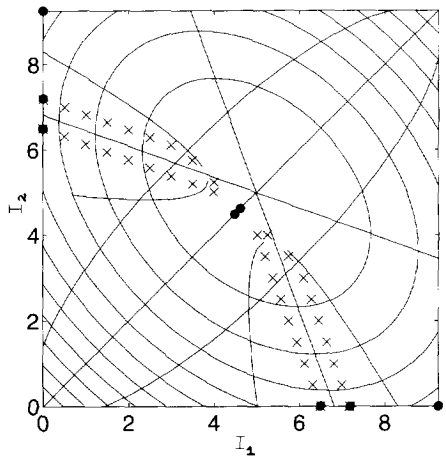

Fig. 1. Classical phase space structure of the Baggot Hamiltonian for H_2O. Primary periodic orbits (•) and resonant 2-tori (×) are shown.

by finding the stationary points of the effectively two-degree-of-freedom Hamiltonian expressed in terms of 2 resonant angles [17,34].

The primary pos appear in 1-parameter families in $(\mathcal{N}, I_1, I_2)$ space; the relevant bifurcation diagram has been computed by Lu and Kellman [17]. Following Lu and Kellman, we have determined the primary pos for the classical Baggot Hamiltonian [34]. The families of pos intersect constant $\mathcal{N}$ planes at *isolated points*, which are marked as circles in Fig. 1. There are 3 pairs of symmetry related ($1 \leftrightarrow 2$) pairs of pos on the I_1 and I_2 axes, respectively (filled circles). Two are pairs of 2:1 bond stretch–bend pos, one stable and one (singly) unstable. The remaining pair consists of a pair of local mode stretch orbits, where all energy is in one or the other bond stretching mode. In addition, pos appear along the diagonal $I_1 = I_2$. For example, for all values of $\mathcal{N}$ there are *two* pos with $I_1 = I_2 = \mathcal{N}/4$ (filled circle), corresponding to stable and unstable (asymmetric and symmetric stretch, respectively) normal mode pos. At $\mathcal{N} = 18.5$, there are two other pos on the diagonal. One (filled circle) lies in the physical region of action space, and is a 2:1 bend/normal mode resonant po; another po lies outside the physical action region, and is also a bend/normal mode po.

We see that, for fixed $\mathcal{N}$, the primary pos appear at isolated points in the action plane. The probability of finding one of the primary pos at an arbitrary value of

the classical energy is zero. The primary pos can thus hardly be said to form the "skeleton" of the classical phase space structure; they are more akin to the joints of the skeleton. To map out the classical phase space structure it is necessary to consider higher dimensional classical objects; such objects are resonance channels, the object of standard Chirikov analysis, and families of resonant 2-tori.

3.2. Chirikov resonance analysis for $\mathcal{H}_0$

Resonance conditions for the Baggot Hamiltonian are determined in the usual way [22] by analyzing $\mathcal{H}_0$. Zeroth order frequencies are

$$\omega_\sigma \equiv \frac{\partial \mathcal{H}_0}{\partial I_\sigma} = \Omega_s + 2\alpha_s I_\sigma + \epsilon_{ss}(1-\delta_{\sigma\sigma'})I_{\sigma'} + \epsilon_{sb} I_b, \quad \sigma = 1,2, \tag{3.1a}$$

$$\omega_b \equiv \frac{\partial \mathcal{H}_0}{\partial I_b} = \Omega_b + 2\alpha_b I_b + \epsilon_{sb} \sum_{\sigma=1,2} I_\sigma. \tag{3.1b}$$

The resonance conditions for the 1:1 and 2:1 cases are obtained by setting $\omega_1(\boldsymbol{I}) = \omega_2(\boldsymbol{I})$ and $\omega_\sigma(\boldsymbol{I}) = 2\omega_b(\boldsymbol{I})$, respectively, yielding immediately the resonance conditions in action space

$$2(\epsilon_{sb} - \alpha_s)I_\sigma + (2\epsilon_{sb} - \epsilon_{ss})I_{\sigma'}(1-\delta_{\sigma\sigma'}) = \Omega_s - 2\Omega_b + (\epsilon_{sb} - 4\alpha_b)I_b, \tag{3.2a}$$

$$I_1 = I_2, \tag{3.2b}$$

for the 2:1 and 1:1 cases, respectively, with $\sigma, \sigma' = 1,2$.

Each of the resonance conditions defines a plane in the 3D action space. These planes intersect the constant $\mathcal{N}$ plane in a line, which defines the center of the resonance channel. All three resonance lines intersect at a point $\boldsymbol{I}^r$, which lies either inside or outside the physically allowed part of the action plane, $I_1 + I_2 \leqslant \mathcal{N}/2$, depending on the value of $\mathcal{N}$. Conservation of $\mathcal{N}$ means that we can eliminate I_b to obtain equations for the resonance lines in terms of I_1 and I_2 (see Ref. [34]).

Resonance channel widths (that is, the maximum extent of the resonant region of phase space surrounding the given resonance line) are estimated by making a canonical transformation to an appropriate set of variables, and expanding the Hamiltonian around the center of the resonance channel to obtain a pendulum form (cf. Ref. [22]; further details are given in Ref. [34]). Resonance lines and corresponding channels are plotted in Fig. 1. The diagonal $I_1 = I_2$ is the 1:1 resonance line; in the absence of any other resonances, the region of phase space inside the associated resonance channel corresponds to normal mode trajectories, the region outside to local mode trajectories. The line $I_1 + I_2 = \text{const}$ is then a projection of the polyad phase sphere for the 1:1 resonance (constant I_b) into the (I_1, I_2) plane. We note that, the 1:1 resonance width actually increases then decreases as the actions I_1, I_2 get larger. The two symmetry related 2:1 resonance zones slope inwards towards the 1:1 resonance zone. In the absence of other resonances, each 2:1 resonance channel is a region of phase space in which the bend mode and one of the local stretch modes are strongly coupled. The widths of the 2:1 resonance channels decrease to zero near the center of the action plane.

Of particular interest for the vibrational dynamics of the H_2O molecule are the regions of phase space where the primary resonance channels intersect. Such intersections are characteristic of the dynamics of multimode systems, giving rise to chaotic classical dynamics [3,19]. For $\mathcal{N} = 18.5$, Chirikov resonance analysis shows that the primary resonance channels hardly intersect; consistent with this is the relative ease with which eigenstates for the $P = 8$ manifold can be assigned (see below). On the other hand, for $\mathcal{N} = 34.5$, three resonance channels intersect in the region around $I_1 = I_2 = 8$, and "mixed" or nominally chaotic states are found in this region [34].

In addition to the primary 1:1 and 2:1 resonance zones, the location of higher-order multimode resonances can also be calculated at the next order of perturbation theory [34].

3.3. Families of resonant 2-tori

Chirikov resonance analysis provides an approximate picture of the phase space structure of the H_2O molecule. It is a perturbative approach in that each resonance coupling term is analysed independently. Moreover, the phase space structure in the vicinity of each resonance line is assumed to be pendulum-like [22]. For systems with weak anharmonicities, there may be ranges of E and $\mathcal{N}$ over which the local phase

space structure is more complicated.

A more refined analysis of the phase space structure involves determination of the location of families of *resonant 2-tori*. Consider the classical H_2O Hamiltonian with a single resonance coupling term. There are in this case 2 ignorable angles, and 2 constants of the motion in addition to the energy; for example, if only the 1:1 resonance coupling term is present, I_b and $I_1 + I_2$ are constants of the motion. The dynamics is then described by a 1 degree of freedom reduced Hamiltonian, and stationary (equilibrium) points of this Hamiltonian correspond to *2-tori* in the full phase space. (In the absence of any coupling, almost all trajectories lie on nonresonant 3-tori.)

At fixed superpolyad number $\mathcal{N}$, the resonant 2-tori appear in continuous one-parameter families, as shown in Fig. 1. For the 1:1 resonant case, there are 2 families of normal mode 2-tori along the diagonal $I_1 = I_2$, and a symmetry related pair of local mode 2-tori along the I_1 and I_2 axes. For the single 2:1 resonant case, there is a family of 2-tori along the line $I_1 + I_2 = \mathcal{N}/2$ associated with zero excitation of the bend mode. In addition, there are two families of resonant 2-tori associated with bend-local resonant motion; these families are marked with crosses in Fig. 1, and are located close to the centers of the 2:1 resonance channels determined via Chirikov analysis.

Two conclusions are evident from our computation of the resonant 2-tori. First, the primary pos appear where families of 2-tori meet. Moreover, the location of the primary pos is given quite accurately by the intersection of the loci of the families of 2-tori determined in the single-resonance approximation. Second, it is apparent that the 2-tori form the "skeleton" of the classical phase space, and in fact follow very closely the Chirikov resonance channels. All this suggests that the Chirikov analysis is meaningful for the Baggot Hamiltonian.

3.4. Poincaré surface of section

In addition to the calculations outlined above, we have computed classical surfaces of section for the Baggot Hamiltonian. These surfaces of section are useful in order to determine the significance of the classical phase space structures discussed above, and also to compare with quantum mechanical phase space (Husimi) distribution functions.

As the Baggot Hamiltonian has one ignorable angle, we can define a 2D surface of section (sos) by plotting $(I_1 - I_2)/2$ and $\theta_1 - \theta_2$ at constant values of a sectioning angle $\phi_2 \equiv \theta_1 + \theta_2 - 4\theta_b$ with $\dot{\phi}_2 > 0$. The value of the ignorable angle conjugate to the superpolyad action ($\mathcal{N}$) is irrelevant. All trajectories in a given sos have the same energy E; for given $\mathcal{N}$ there is a range of possible sos energies. Several classical sos are shown in Figs. 2, 3 and 4, all for $\mathcal{N} = 18.5$. The sos energy for each plot is chosen to equal the quantum energy of the state in the $P = 8$ manifold whose Husimi function contours are superimposed.

The general structure of the classical sos is as follows: a normal-mode resonant region is present in the middle of the sos ($I_1 \sim I_2$), corresponding to "librational" motion [3]. Local mode (above barrier) regions are found above and below the central normal mode region. Large 2:1 bend/local-stretch resonant islands appear in the local mode regions (e.g., Fig. 2). Higher-order resonances also appear. For arbitrary values of E, the center of the normal mode islands correspond to stable resonant 2-tori; a "whiskered" (unstable) 2-torus appears at the center of the sos. Similarly, the 2:1 bend/local-stretch resonance is defined by the intersection of stable and unstable resonant 2-tori with the sos.

4. Assignment of eigenstates and the classical–quantum correspondence

Quantum eigenfunctions were generated by diagonalizing the Baggot Hamiltonian for a given polyad number P in the number basis $|n_1, n_2, n_b\rangle$, where n_1, n_2 are the quantum numbers for the anharmonic local O-H stretch modes and n_b denotes the bend quantum number. The local mode Hamiltonian is block diagonal in P and the total number of states at fixed P is $(P+1)(P+2)/2$. In the following, we discuss the manifold of 45 states with $P = 8$. Larger values of P and the details of our various computations including discussion of delocalization of eigenstates in action space are described elsewhere [34].

We focus here on eigenstate phase space (Husimi) distribution functions [31]. We compute a Husimi function for each eigenstate as a function of the pair of variables $(I_1 - I_2)/2$ and $(\theta_1 - \theta_2)$; the resulting phase space density can then be compared directly

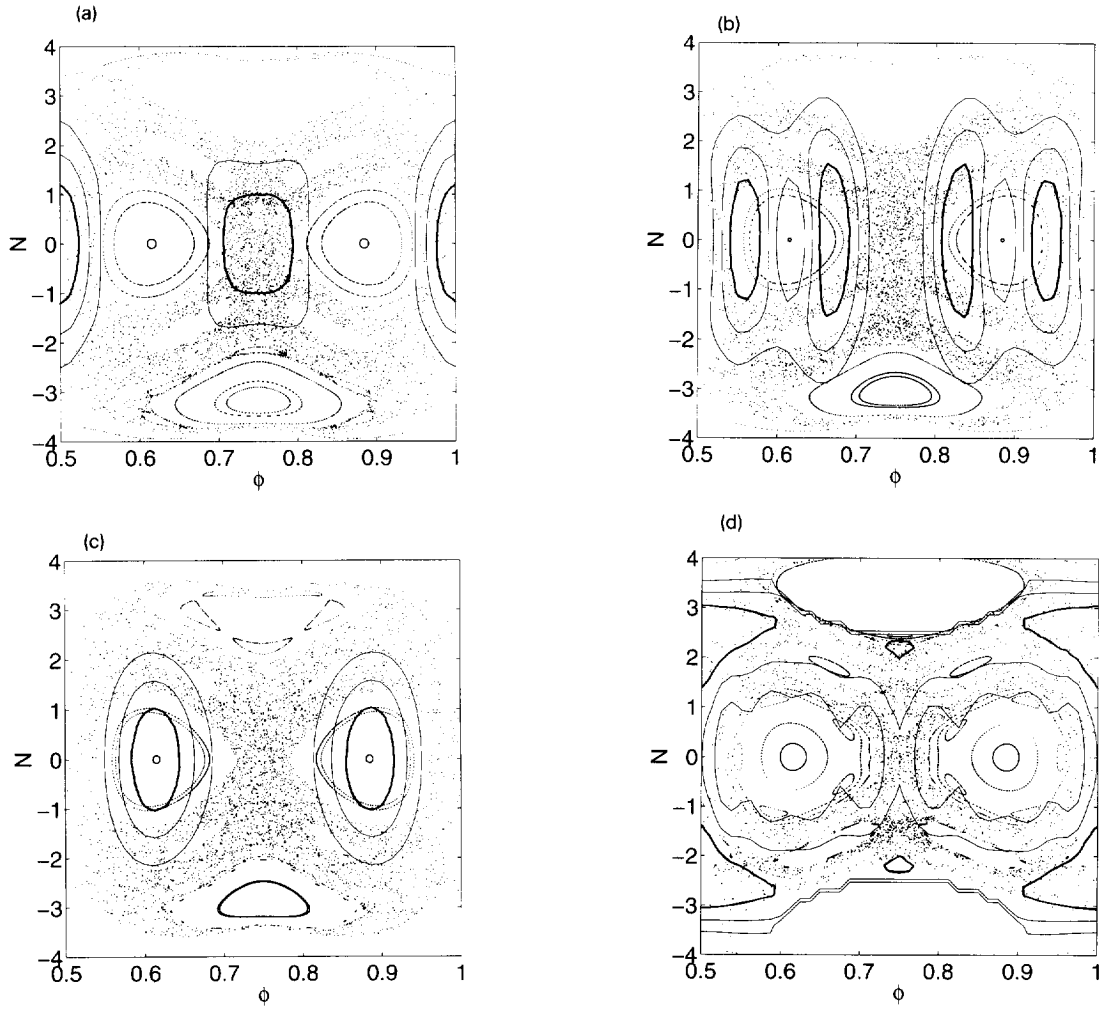

Fig. 2. Classical surfaces of section and quantum mechanical Husimi functions for the Baggot Hamiltonian. (a–c) Sequence of three normal mode states. (d) Local mode state.

with the classical sos.

Our Chirikov resonance analysis of the Baggot Hamiltonian suggests the existence of four classes of eigenstate (cf. Ref. [23]): (1) Nonresonant states, unaffected by any primary resonance. Such states are located in action space outside any of the resonance channels, and good quantum numbers are the zeroth-order quantum numbers n_1, n_2 and n_b. (2) Normal mode (1:1) resonant states, located in the 1:1 resonance channel. Approximate good quantum numbers are $\mathcal{N}$, $\mathcal{N}_{12} = n_1 + n_2$ and a third quantum number ν describing the level of excitation inside the 1:1 resonance. (3) Local-bend resonant states, located in the 2:1 resonance channel. Good quantum numbers are $\mathcal{N}$, $\mathcal{N}_{\sigma b} = 2n_\sigma + n_b$, and a resonant excitation quantum number ν. (4) "Mixed" or nominally "chaotic" eigenstates, located at the resonance channel intersection [34].

For $P = 8$, examination of eigenstate Husimi distributions shows that *almost all states can be assigned to one of the first 3 classes.* In fact, only 2 states out of the 45 could conceivably be labelled as strongly mixed, and these 2 states are involved in an isolated avoided crossing (see below). For the $P = 8$ mani-

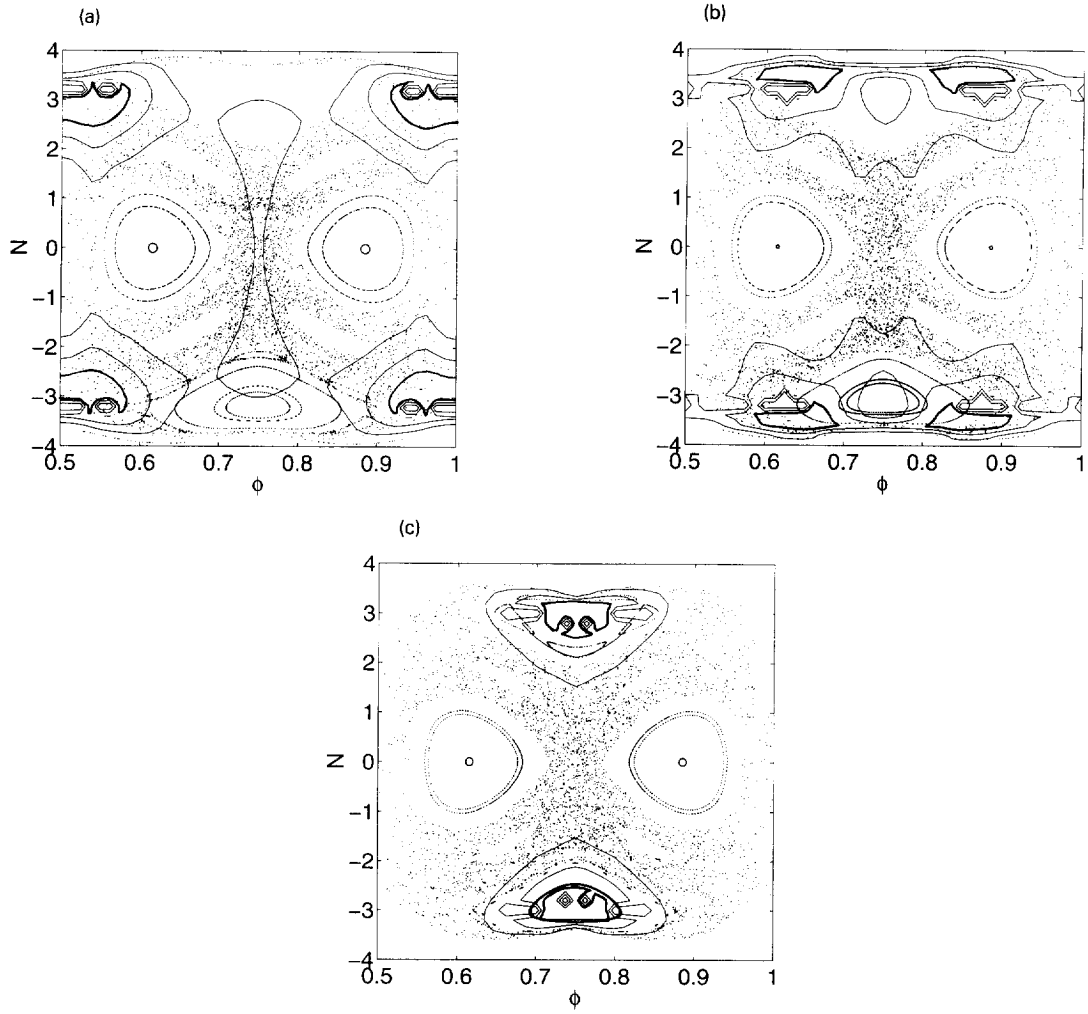

Fig. 3. Classical surfaces of section and quantum mechanical Husimi functions for the Baggot Hamiltonian. (a–c) Sequence of three local-stretch/bend resonant states.

fold of H_2O, we therefore conclude that *there are no "chaotic" states* (compare with Ref. [15]). Strongly mixed states do however appear at higher values of P.

It is important to note that our assignment of states as resonant or nonresonant is based ultimately upon a comparison of quantum and classical phase space distributions, not upon the location of the state in action space. Moreover, the resonances in question are large primary resonances (1:1 and 2:1). The relation between classical and quantum resonance has been discussed by Roberts and Jaffé [29] and by Ramachandran and Kay [35].

We now provide examples of each kind of state. In Fig. 2 we show Husimi function contours superimposed on corresponding classical sos for 4 eigenstates of the Baggot Hamiltonian. Three of the eigenstates form a sequence of (+) parity normal mode states with $\mathcal{N}_{12} = 4$ and $\nu = 0$ (Fig. 2c), 1 (Fig. 2b) and 2 (Fig. 2a), respectively. For these states the phase space density is localized either inside the 1:1 resonance zone (Figs 2b and 2c) or on the unstable normal mode 2-torus (Fig 2a). The fourth eigenfunction is a local mode state, with $(n_1, n_2) \simeq (4, 0)$. The Husimi function is localized outside the 1:1 resonance zone,

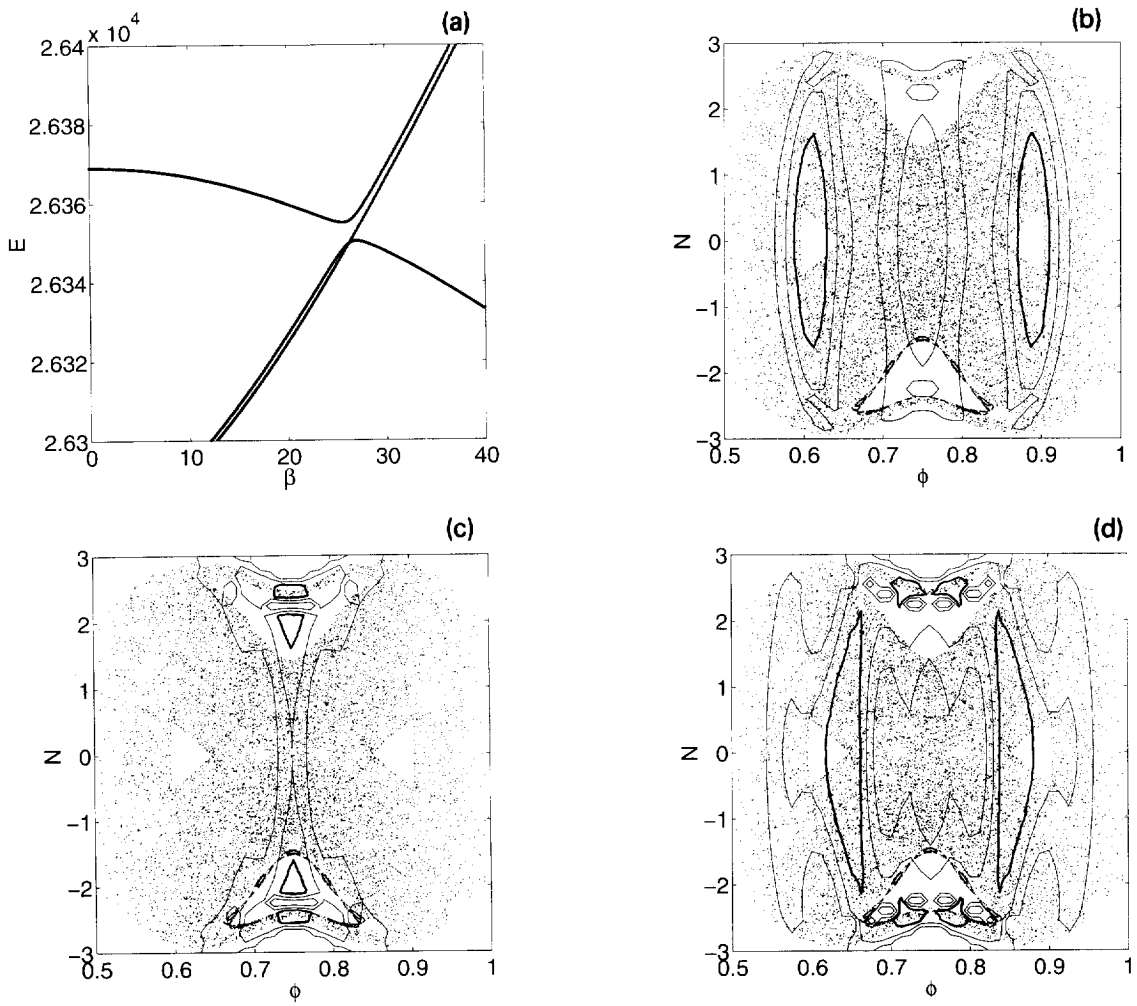

Fig. 4. State mixing and a narrowly avoided crossing. (a) Eigenvalues as a function of stretch–bend coupling strength β_{sb}. Two states ((−) local-stretch/bend resonant and normal) interact; a third ((+) local-stretch/bend resonant) is unaffected. (b–d) Classical surfaces of section and Husimi distribution functions for eigenstates involved (see text).

and is distorted by the presence of the 2:1 resonance channel.

In Fig. 3 we show a sequence of three (+) parity states that are assigned as local stretch/bend resonance states with $2n_\sigma + n_b = 16$ and $\nu = 0$ (3c), 1 (3b) and 2 (3a). The state in Fig. 3c is localized at the center of the 2:1 resonance channel; the state in Fig. 3b is an excited state that lies near the boundary of the resonance zone, while the state in Fig. 3a is localized on the unstable 2:1 resonant 2-torus.

Finally, in Fig. 4 we analyze the two most "mixed" states in the $P = 8$ manifold. The correlation diagram in Fig. 4a shows that, at the physical value of the stretch–bend coupling parameter β_{sb}, the two (-) parity states whose Husimis are shown in Figs 4b and 4d are involved in an avoided crossing. The third state, shown in Fig. 4c, is a (+) parity 2:1 resonant state, and is the partner of one of the two interacting states. The other state involved in the avoided crossing is a normal mode (1:1 resonant) state. The greatest amount of mixing seen in the $P = 8$ manifold thus corresponds to the 2-state interaction seen in Fig. 4. One interpretation of the mixing is an enhanced dynamical tunnelling [4] of the resonant doublet induced by the

delocalized normal mode state.

5. Conclusions

In this Letter we have studied the classical and quantum mechanics of the Baggot vibrational Hamiltonian for H_2O [16]. We have shown first of all that standard Chirikov resonance analysis provides a useful approximate map of the classical phase space. This conclusion is supported by more rigorous analysis of classical phase space structure in terms of families of resonant 2-tori, and by examination of classical surfaces of section. We point out that determination of the location of primary periodic orbits alone is not sufficient to understand the phase space structure of the Baggot Hamiltonian.

We have also examined quantum phase space (Husimi) distribution functions for eigenstates of the Baggot Hamiltonian. For the manifold of states examined (all states with $P = 8$), it is found that almost all states can be assigned as belonging to one of 3 distinct types of eigenstates; these assignments are made with the aid of the Husimi function. Only 2 states could conceivably be described as strongly mixed, and these states are found to be involved in a 2-state avoided crossing. Therefore, in contrast to the analysis of Lu and Kellman [15], we do not find any "chaotic" states. Highly mixed states in the vicinity of the intersection of classical resonance channels are however found for larger values of P which will be discussed elsewhere [34].

Acknowledgement

This work supported by NSF Grant CHE-9403572. Computations reported here were performed in part on the Cornell Supercomputer Facility, which is supported by NSF and IBM corporation.

References

[1] C.E. Hamilton, J.L. Kinsey and R.W. Field, Ann. Rev. Phys. Chem. 37 (1986) 493.
[2] K.K. Lehmann, G. Scoles and B.H. Pate, Ann. Rev. Phys. Chem. 45 (1994) 241, and references therein.
[3] A.J. Lichtenberg and M.A. Lieberman, Regular and stochastic motion (Springer, Berlin, 1983).
[4] M.J. Davis and E.J. Heller, J. Phys. Chem. 75 (1981) 246.
[5] R.L. Sundberg, E. Abramson, J.L. Kinsey and R.W. Field, J. Chem. Phys. 83 (1985) 466.
[6] M.J. Davis, Int. Rev. Phys. Chem. 14 (1995) 15.
[7] J.M. Gomez Llorente and E. Pollak, Ann. Rev. Phys. Chem. 43 (1992) 91, and references therein.
[8] M.A. Sepulveda and F. Grossmann, Adv. Chem. Phys. (preprint, 1996), and references therein.
[9] M.E. Kellman, in: Molecular dynamics and spectroscopy by stimulated emission pumping, ed. H.-L. Dai and R.W. Field (World Scientific, Singapore, 1995).
[10] D.A. Sadovskii and B. Zhilinskii, Phys. Rev. A 48 (1993) 1035, and references therein.
[11] C. Jaffé, J. Chem. Phys. 89 (1988) 3395.
[12] M.E. Kellman and E.D. Lynch, J. Chem. Phys. 89 (1988) 3396.
[13] M. Joyeux, Chem. Phys. 203 (1996) 281.
[14] G.S. Ezra, J. Chem. Phys. 104 (1996) 26, and references therein.
[15] Z.-M. Lu and M.E. Kellman, Chem. Phys. Lett. 247 (1995) 195.
[16] J.E. Baggot, Mol. Phys. 65 (1988) 739.
[17] Z.-M. Lu and M.E. Kellman, submitted for publication (cited in Ref. [15]).
[18] R. Mackay, J.D. Meiss and I.C. Percival, Physica D 13 (1984) 55.
[19] S. Wiggins, Normally hyperbolic invariant manifolds in dynamical systems (Springer, Berlin, 1994), and references therein.
[20] R.E. Gillilan and G.S. Ezra, J. Chem. Phys. 94 (1991) 2648.
[21] V.I. Arnold, Russ. Math. Survey 18 (1963) 85.
[22] B.V. Chirikov, Phys. Rep. 52 (1979) 263.
[23] D.W. Oxtoby and S.A. Rice, J. Chem. Phys. 65 (1976) 1676.
[24] C. Jaffé and P. Brumer, J. Chem. Phys. 73 (1980) 5646.
[25] C.C. Martens, M.J. Davis and G.S. Ezra, Chem. Phys. Lett. 142 (1987) 519.
[26] Y.M. Engel and R.D. Levine, Chem. Phys. Lett. 164 (1989) 270.
[27] C.C. Martens, J. Stat. Phys. 68 (1992) 207.
[28] K.M. Atkins and D.E. Logan, Phys. Lett. A 162 (1992) 255.
[29] F.L. Roberts and C. Jaffé, J. Chem. Phys. 99 (1993) 2495.
[30] J. Laskar, C. Froeschlé and A. Celletti, Physica D 56 (1992) 253.
[31] K. Husimi, Proc. Phys. Math. Soc. Japan 22 (1940) 264.
[32] L.E. Fried and G.S. Ezra, J. Chem. Phys. 86 (1987) 6270.
[33] M.E. Kellman, J. Chem. Phys. 93 (1990) 6630.
[34] S. Keshavamurthy and G.S. Ezra, to be submitted.
[35] B. Ramachandran and K.G. Kay, J. Chem. Phys. 99 (1993) 3659.